Adsorption (2012) 18:359–366
DOI 10.1007/s10450-012-9414-2

# NMR studies of carbon dioxide and methane self-diffusion in ZIF-8 at elevated gas pressures

**Anne-Kristin Pusch · Tobias Splith · Lutz Moschkowitz · Shilpi Karmakar · Rajesh Biniwale · Marco Sant · Giuseppe B. Suffritti · Pierfranco Demontis · Janosch Cravillon · Evangelia Pantatosaki · Frank Stallmach**

Received: 22 May 2012 / Accepted: 31 August 2012 / Published online: 20 September 2012


**Abstract** Self-diffusion measurements with methane and carbon dioxide adsorbed in the Zeolitic Imidazolate Framework-8 (ZIF-8) were performed by $^{1}H$ and $^{13}C$ pulsed field gradient nuclear magnetic resonance (PFG NMR). The experiments were conducted at 298 K and variable pressures of 7 to 15 bar in the gas phase above the ZIF-8 bed. Via known adsorption isotherms these pressures were converted to loadings of the adsorbed molecules. The self-diffusion coefficients of carbon dioxide measured by PFG NMR are found to be independent of loading. They are in good agreement with results from molecular dynamic (MD) simulations and resume the trend previously found by IR microscopy at lower loadings. Methane diffuses in ZIF-8 only slightly slower than carbon dioxide. Its experimentally obtained self-diffusion coefficients are about a factor of two smaller than the corresponding values determined by MD simulations using flexible frameworks.

A.-K. Pusch · T. Splith · L. Moschkowitz · F. Stallmach (✉)
Faculty of Physics and Earth Sciences, University Leipzig, Linnestraße 5, 04103 Leipzig, Germany
e-mail: stallmac@physik.uni-leipzig.de

S. Karmakar · R. Biniwale
National Environmental Engineering Research Institute (NEERI), Nagpur, India

M. Sant · G.B. Suffritti · P. Demontis
Department of Chemistry, University of Sassari, Sassari, Italy

J. Cravillon
Institute of Inorganic Chemistry, University Hannover, Hannover, Germany

E. Pantatosaki
School of Chemical Engineering, National Technical University of Athens, Athens, Greece

**Keywords** ZIF-8 · Self-diffusion · Carbon dioxide · Methane · NMR · Molecular dynamic simulation

## 1 Introduction

Zeolitic Imidazolate Frameworks (ZIF) are a subfamily of metal organic frameworks (MOF) (Park et al. 2006). Generally, ZIF's are composed of transition metal-clusters and imidazole as organic linkers. They are microporous crystalline materials, which resemble structure types known from inorganic zeolites. Like other MOFs, the ZIFs are characterized by a tunable pore size. For a few of the ZIF structures, high chemical and thermal stabilities of up to 550 °C were reported (Park et al. 2006; Basu et al. 2011). This opens up a wide field for potential applications as high-tech material in adsorption and separation technologies (Wang et al. 2008; Liu et al. 2009, 2011; Venna and Carreon 2010; Bux et al. 2010, 2011).

For an optimal characterization of porous materials for gas separation, it is crucial to know the adsorption and transport properties of molecules in the pore system (Li et al. 2009; Ferey et al. 2011; Atci et al. 2011). Experimental methods that are frequently used to measure molecular diffusion in modern MOF materials involve quasi elastic neutron scattering (QENS) (Deroche et al. 2011; Yang et al. 2011), pulsed field gradient (PFG) NMR (Stallmach et al. 2006; Wehring et al. 2010), infrared microscopy and interference microscopy (Bux et al. 2010). Transport processes in the MOFs are also often studied by molecular dynamic (MD) computer simulations (Liu et al. 2011; Keskin et al. 2009; Sant et al. 2010; Zheng et al. 2012; Pantatosaki et al. 2010, 2012). Since computer simulations

do not require the synthesis of the porous materials for the experiments, they are in particular useful for screening MOF's with respect to potentially interesting gas separation properties. Additionally, if combined and validated with experimental diffusion studies, MD simulations may provide unique insight into the transport mechanisms at the pore level scale. Recent examples for such joint experimental and computational investigations include diffusion studies of *n*-alkanes in MIL-47 (Deroche et al. 2011) and MOF-5 (Ford et al. 2012), benzene in MOF-5, methane in CuBTC (Wehring et al. 2010) and methane and carbon dioxide in UiO-66 (Yang et al. 2011).

Due to its potential application as active membrane material for biogas or natural gas purification, methane and carbon dioxide diffusion in ZIF-8 is of particular interest (Venna and Carreon 2010; Bux et al. 2010; Basu et al. 2011; Dai et al. 2012). Computer simulation studies were performed to predict adsorption and/or diffusion of hydrogen, methane and carbon dioxide in ZIF-8 (Liu et al. 2009, 2011; Hertaeg et al. 2011). First experimental diffusion studies for this system were obtained by infrared microscopy (IRM) (Bux et al. 2010). In IRM, the time dependence of intracrystalline concentration profiles of adsorbed molecules during gas uptake were measured on large single-crystals of ZIF-8. From these non-equilibrium data, transport diffusion coefficients of methane and carbon dioxide were derived. Further analysis using adsorption isotherms provided corrected diffusion coefficients and separation factors for methane and carbon dioxide gas mixtures, which generally compared well to predictions from molecular simulation. Single component IRM diffusion studies were performed in the loading range of up to 2 molecules per cage for methane and up to about 5 molecules per cage for carbon dioxide (Bux et al. 2010), corresponding to pressures in the gas phase of up to about 8 bar.

Recently, we published first experimental results of carbon dioxide and methane self-diffusion in ZIF-8 obtained by using $^{13}C$ and $^{1}H$ PFG NMR, respectively. The results, which were only available for one loading, were found to be consistent with IRM data and MD simulations (Pantatosaki et al. 2012). In the present study, we investigated the loading dependence of single component methane and carbon dioxide self-diffusion by PFG NMR and MD simulations. Compared to available IRM data (Bux et al. 2010), we extended the loading range to higher loadings and thus higher pressures in the gas phase. The results are compared to published experimental and MD simulation data. They provide a more comprehensive knowledge of the single component diffusional behavior of these two guest molecules in ZIF-8.

## 2 Materials and methods

### 2.1 ZIF-8 material

PFG NMR self-diffusion studies require beds of crystalline ZIF-8 material of about 100 mg per NMR sample. The crystal size may be substantially smaller than required for the IRM studies with large single crystals. However, it should also exceed 10 to 20 μm in diameter in order to be able to measure intracrystalline self-diffusion. The required amounts and qualities of ZIF-8 for preparing sets of samples to study the loading dependence of self-diffusion were obtained from University Hannover (Germany) and NEERI (India).

Intermediate sized ZIF-8 crystals in sufficient amounts for NMR studies were synthesized by University Hannover in the following way: $ZnCl_2$, 2-methyle-imidazole (Hmim) and $NaHCO_2$ were dissolved in 500 mL of MeOHA. All chemicals were obtained from Sigma-Aldrich. A clear solution is prepared with a molar ratio $Zn/Hmim/NaHCO_2/MeOH = 1 : 2 : 2 : 250$. The solution is treated without stirring at 373 K for 24 h in a sealed glass tube under homogeneous heating in a convection oven. The crystals are recovered by filtration with a 20 μm sieve to get rid of the smaller crystals, washed with MeOH and dried under reduced pressure. A detailed description of the synthesis and the characterization of the ZIF-8 material obtained may be found in Refs. (Cravillon et al. 2012; Bux et al. 2009).

The ZIF-8 from NEERI was synthesized in a similar procedure as reported by Park et al. (2006). A mixed solution of $Zn(NO_3)_2\ 6H_2O$ (2.1 g) and 2-methyle-imidazole (0.6 g) was prepared by dissolving in 360 ml dimethyl formamide (DMF). A through mixing was achieved by stirring the solution for 1 h using a rotary shaker. Solvothermal synthesis was carried out using a sealed glass bottle by heating in an oven at 140 °C for 24 h. Subsequently, the product mixture was allowed to cool down to room temperature. Crystals were obtained in the solution and at the walls of the bottle. The product was filtered and dried in air for 10 min. In order to remove any residual solvent, the material was then washed with chloroform and dried at 85 °C for 30 min. The dried sample was first calcined at 200 °C for 1 h following at 300 °C for 2 h in vacuum.

XRD analysis of ZIF-8 after calcination at 300 °C was performed with a Rigaku Miniflex II X-ray diffractometer within a $2\theta$ range of 10° to 50° using Cu-K$\alpha$ radiation ($\lambda = 0.15418$ nm). The XRD pattern shown in Fig. 1 matches well with the reported pattern for ZIF-8 (Park et al. 2006). The SEM investigations were carried out by a JEOL JSM-6380-A instrument using 10.0 kV acceleration voltages. Well defined large crystals of ZIF-8 were obtained. An example is shown in Fig. 2. Smaller particles were formed

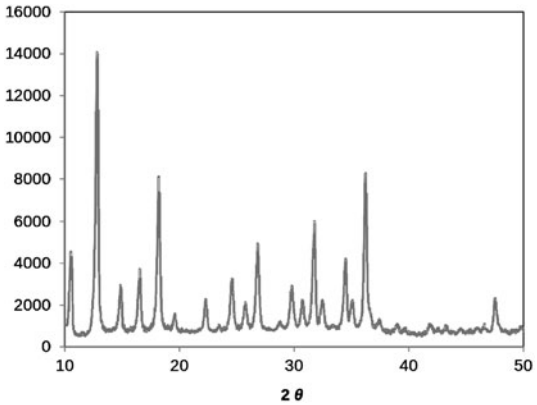


**Fig. 1** XRD pattern of ZIF-8 for the sample calcined at 300 °C

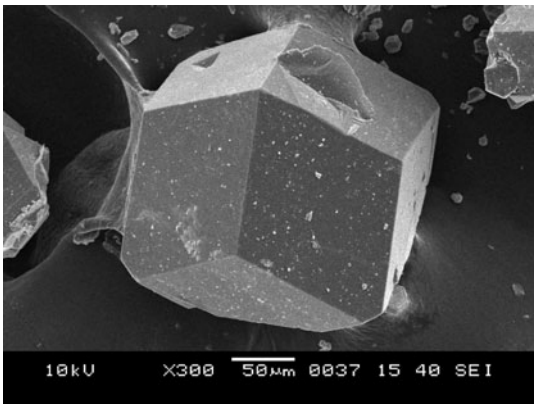


**Fig. 2** SEM micrograph of ZIF-8 showing a well shaped large crystal with a diameter of about 150 µm. Smaller crystals are visible at the edges of the micrograph

as well. A part of the crystals was crushed due to sample removal from glass walls. The defects are visible on the crystal surface.

With respect to standard characterizations, there is no indication that the ZIF-8 materials from both sources have significantly different properties. Since for NMR sample preparation (see below), the knowledge of adsorption isotherms at elevated pressures in ZIF-8 is essential, the quality of both ZIF-8 samples is proved by comparison of their carbon dioxide and methane adsorption behavior.

Figure 3 shows measured single component adsorption isotherms for carbon dioxide and methane at low pressures (0.01 bar to 1 bar) with ZIF-8 from NEERI and at high pressures (1 to 20 bar) with ZIF-8 from University Hannover. The data are compared to recently published data for ZIF-8 (Perez-Pellitero et al. 2010) covering a similar elevated pressure range. The measurements show that at the same pressure the ZIF-8 adsorbs more carbon dioxide than methane. Moreover, although the investigated ZIF-8 samples originate from different sources, the carbon dioxide and methane adsorption isotherms obviously follow the same trend and agree within the experimental uncertainties. Thus, at least

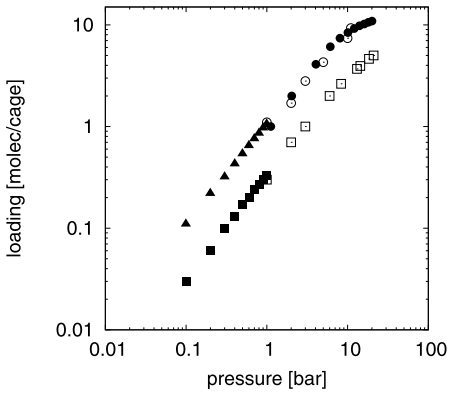


**Fig. 3** Adsorption isotherms for $CO_2$ and $CH_4$ in ZIF-8 at room temperature. Comparison of $CO_2$ data measured at low pressures (▲, ZIF-8 from NEERI) and at elevated pressures (●, ZIF-8 from University Hannover) with previously published data (○, Perez-Pellitero et al. 2010). Methane data at low pressures (■, ZIF-8 from NEERI) compared to data from Perez-Pellitero et al. (2010) (□)

with respect to their adsorption properties, the equivalence of the ZIF-8 materials used in this study is confirmed.

## 2.2 NMR sample preparation

In order to cover the high loading range for methane and carbon dioxide in ZIF-8, NMR measurements had to be performed at elevated pressures in the gas phase. For this purpose, thick-walled glass tubes with an outer diameter of 10 mm and a wall thickness of 1.5 mm were used.

For each sample an amount of about 110 mg of ZIF-8 was filled into these NMR sample tubes. To activate the samples, the ZIF-8 beds in the sample tubes were slowly heated in vacuum up to a temperature of 393 K. The temperature was maintained for 12 h to completely remove residual solvents, gases and moisture from the pore space. After controlled cooling down to room temperature, the single-component adsorption was performed by exposing the activated ZIF-8 to volumetrically determined amounts of $CO_2$ (99 % $^{13}$C-enriched, Sigma-Aldrich) and $CH_4$, respectively.

The required amounts of the adsorbate gases were determined using single-component adsorption isotherms as published in Perez-Pellitero et al. (2010) and shown in Fig. 3. The gases were frozen into the sample tube by chilling the ZIF-8 bed to about 77 K using liquid nitrogen. Finally, the glass tubes were sealed by ablating them a few centimeters above the MOF bed.

## 2.3 NMR measurements

The self-diffusion of methane and carbon dioxide adsorbed in ZIF-8 was investigated at 298 K by $^1$H and $^{13}$C PFG NMR. The experiments with adsorbed methane were carried out using the NMR spectrometers FEGRIS NT and FT

equipped with home-built $z$-gradient systems for diffusion studies (Stallmach and Galvosas 2007). These spectrometers operate at a proton ($^1$H) resonance frequency of 125 MHz and 400 MHZ, respectively. The $^{13}$C NMR studies were carried out only at the FEGRIS FT NMR spectrometer (Stallmach and Galvosas 2007) at 100.6 MHZ resonance frequency using the $z$-gradient and probe system, described in Schlayer et al. (2012).

The PFG NMR diffusion studies in the porous systems were performed using the 13-interval pulse sequence (Stallmach and Galvosas 2007; Cotts et al. 1989). Pulsed field gradient amplitudes $G$ of up to 5 T m$^{-1}$ and gradient pulse lengths of $\delta = 1.2$ ms were applied to achieve a sufficient spin echo attenuation. The rf pulse separation was chosen to be $\tau = 4$ ms. The 13-interval pulse sequence was applied since it minimizes disturbing influences of constant internal background gradients and of cross terms with the applied pulsed field gradients on the observed spin echo attenuation. Observation times $\Delta$ were chosen from $\Delta = 20$ ms to 80 ms. These values are much smaller than the measured longitudinal relaxation times ($T_1 \gg \Delta$). In this way, a relaxation time weighting of the observed PFG NMR spin echo attenuations and of the determined self-diffusion coefficients was prevented.

To obtain the self-diffusion coefficients from the observed spin echo attenuation $\Psi$, a bi-exponential model was applied

$$\Psi = \frac{M(b)}{M_0} = (1-p)\cdot\exp(-bD_1) + p\cdot\exp(-bD_2), \quad (1)$$

where $M(b)$ denotes the NMR signal intensity as a function of the $b$-value (Stallmach and Galvosas 2007). For the 13-interval pulse sequence, it is given by $b = (2\gamma\delta G)^2(\Delta - \frac{1}{6}\delta - \frac{1}{2}\tau)$ (Stallmach and Galvosas 2007; Cotts et al. 1989). A bi-exponential behavior as in Eq. (1) was found for all measurements with the ZIF-8 samples indicating fast self-diffusion in the gas phase ($D_1$) between the ZIF-8 crystals in the bed and slower intracrystalline self-diffusion in the adsorbed phase ($D_2$). The value $p$ denotes the relative amount of diffusing molecules, which diffuse in the adsorbed intracrystalline space.

To verify the actual pressures and loadings in the sealed NMR samples, $T_1$ relaxation measurements in the pure gas phase above the ZIF-8 crystal bed were conducted. The relaxation times in the gas phase above the ZIF-8 bed were compared to known pressure dependent $CO_2$ gas phase relaxation times published in Etesse et al. (1992).

### 2.4 MD simulations

Using various force fields for ZIF-8 (details see Pantatosaki et al. 2012; Zheng et al. 2012), molecular dynamic simulations of carbon dioxide and methane in a flexible ZIF-8 framework were performed. For $CO_2$ in particular, one of the force fields uses the partial charges obtained via accurate ab-inito computations by Rana et al. (2011). The mean squared displacements (MSD) were calculated for different sorbate loadings. Generally, at short times there is a fast intra-cage diffusivity, until the sorbate molecules reach the walls of the cage. During these short times the MSD increases fast. After about 40 ps the MSD increase slows down and becomes linear with the time. Fitting a straight line for this final part of the MSD curve, the sorbate self-diffusivity was obtained. MD simulations were performed for different carbon dioxide and methane loadings.

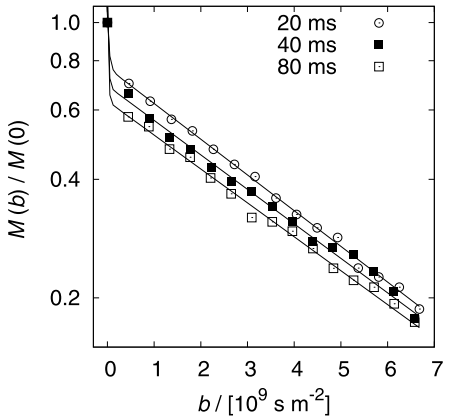


**Fig. 4** $^{13}$C PFG NMR spin echo attenuation for carbon dioxide adsorbed in ZIF-8 at 15 bar for three different observation times (see legend). Data were fitted using Eq. (1). The slowly decaying second part represents the intracrystalline self-diffusion, which obviously does not depend on observation time

## 3 Results and discussion

Figure 4 shows a representative example of $^{13}$C NMR spin echo attenuation curves observed for carbon dioxide in a ZIF-8 sample at 15 bar (corresponding to about 10 molecules per cage). The lines represent fits according to Eq. (1). The fast decay at small $b$ values is caused by the fast diffusion in the gas phase between the ZIF-8 crystals in the bed. Due to the elevated pressure and thus increased carbon dioxide density in the gas phase, there is a significant NMR signal contribution from the gas, which is rarely observed in PFG NMR. For larger $b$ values, the curve decays slower and the slope becomes independent of observation time (curves for different observation time run in parallel). This is the finger print of time-independent intracrystalline self-diffusion through the pore space of the porous host. An intracrystalline self-diffusion coefficient of adsorbed carbon dioxide of $D_2 = (2.2 \pm 0.1) \times 10^{-10}$ m$^2$ s$^{-1}$ was determined from the fit using Eq. (1). At the largest observation time of 80 ms, this corresponds to a diffusion length (root mean square displacement) of less then about 10 µm. This is small

**Table 1** Self-diffusion coefficients for $CO_2$ and $CH_4$ in ZIF-8 determined by PFG NMR ($D_{NMR}$, this work) and obtained by MD simulations ($D_{MD}$, ref.)

| | Pressure [bar] | Loading [mg/g] | Loading [molec/cage] | $D_{NMR}$ [$m^2/s$] | $D_{MD}$, ref. [$m^2/s$] |
|---|---|---|---|---|---|
| $CO_2$ | 28 | 350 | 12.0 | $1.4 \times 10^{-10}$ | |
| | 15 | 286 | 10.0 | $2.2 \times 10^{-10}$ | |
| | 11 | 245 | 8.9 | $2.2 \times 10^{-10}$ | |
| | 10 | 252 | 8.4 | $2.1 \times 10^{-10}$ | $3.9 \times 10^{-11}$ (Battisti et al. 2011) |
| | 9 | 205 | 7.7 | $1.7 \times 10^{-10}$ | |
| | 8 | 227 | 7.4 | $2.1 \times 10^{-10}$ | |
| $CH_4$ | 14 | 44 | 4.0 | $1.4 \times 10^{-10}$ | |
| | 12 | 40 | 3.7 | $1.3 \times 10^{-10}$ | $1.9 \times 10^{-10}$ (Hertaeg et al. 2011) |
| | 10 | | | | $1.8 \times 10^{-9}$ (Battisti et al. 2011) |
| | 9 | 33 | 2.7 | $1.2 \times 10^{-10}$ | |
| | 7 | 25 | 2.1 | $8.8 \times 10^{-11}$ | |

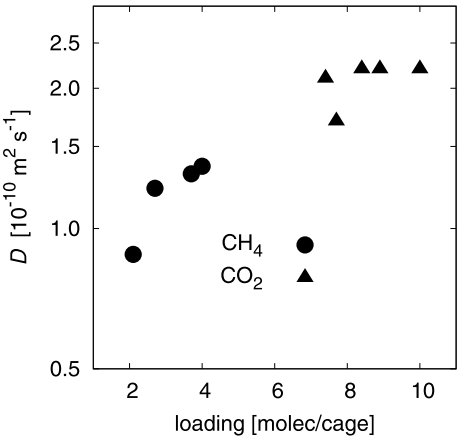


**Fig. 5** Self-diffusion coefficients of methane and carbon dioxide as obtained by PFG NMR. The loadings are given in molecules per cage of ZIF-8 and cover for both gases a pressure range of about 7 to 15 bar. See also Table 1

compared to crystal sizes, which confirms that intracrystalline self-diffusion is observed in these experiments.

Figure 5 and Table 1 summarize the experimental NMR results for the intracrystalline self-diffusion coefficients of methane and carbon dioxide. The data are presented in dependence on loading (molecules per cage) in Fig. 5 and on loading and the corresponding pressure in the gas phase in Table 1. Since the adsorption capacities for carbon dioxide exceed those for methane at the same pressure (see Fig. 3 and Ref. (Perez-Pellitero et al. 2010)), the adsorbed amounts are different while the pressure ranges are similar.

The self-diffusion coefficients of methane in ZIF-8 are in the range of $8.8 \times 10^{-11}$ to $1.4 \times 10^{-10}$ $m^2\,s^{-1}$. They show a tendency to increase with loading. With the exception of some scatter in the experimental data, the carbon dioxide diffusivity is slightly higher than that of methane but remains nearly constant for loadings between 7 and 12 molecules per cage. Only at the highest pressure of 28 bar (about 12 molecules per cage) the carbon dioxide self-diffusion coefficient decrease slightly (see Table 1). Gate opening effects, as e.g. recently discussed for adsorption investigations in ZIF-7 and ZIF-8 (Fairen-Jimenez et al. 2011; Aguado et al. 2011), are not evident in the study of methane and carbon dioxide mobility presented here. However, at 298 K framework flexibility is obviously present which ensures that the bulkier methane molecules (kinetic diameter of 3.8 Å) can move through the narrow windows of ZIF-8 (window diameter 3.4 Å) with a self-diffusion coefficient comparable to the heavier and smaller carbon dioxide molecules (kinetic diameter of 3.3 Å). In this way, also the small difference between the diffusivities of the carbon dioxide and methane may be understood as a size effect. The smaller carbon dioxide molecule experiences less restrictions as the bulkier methane when passing through the narrow windows of the ZIF-8.

Figure 6 compares the NMR self-diffusion coefficients for methane with previously reported experimental diffusivities obtained by infrared microscopy (IRM) using large single crystals of ZIF-8 (Bux et al. 2010) and with molecular dynamic simulations (Pantatosaki et al. 2012). Further comparisons with MD simulation results are provided in Table 1. All experimental and simulation data are in the same order of magnitude, showing the consistency between the different methods. This is important, since the investigations were performed with different ZIF-8 samples, under equilibrium (NMR) and non-equilibrium (IRM) experimental conditions and using different force fields and different realizations of flexibility in the framework of ZIF-8 (MD). Extrapolating the NMR data to small loadings, there is even a very good agreement between the experimental NMR and IRM values. At loadings of about 3 to 4 molecules per cage, the self-diffusion coefficients measured by NMR are only slightly smaller than the MD simulations reported by Hertaeg et al. (2011) and by Battisti et al. (2011), thus confirming the simulation models (see Table 1). Our own MD simulations

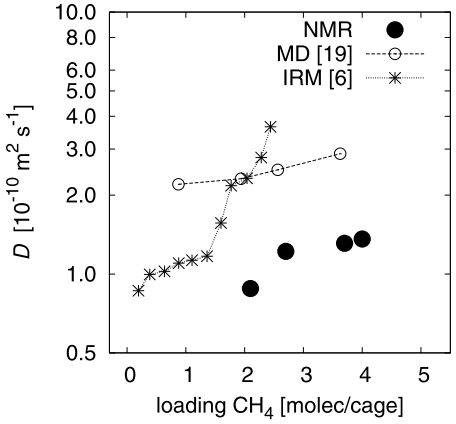


**Fig. 6** Comparison of self-diffusion coefficients of methane determined by PFG NMR (•, this work) with results of MD simulations (○, Pantatosaki et al. 2012) and corrected diffusivities from IRM (∗, Bux et al. 2010). The lines serve as guide for the eyes

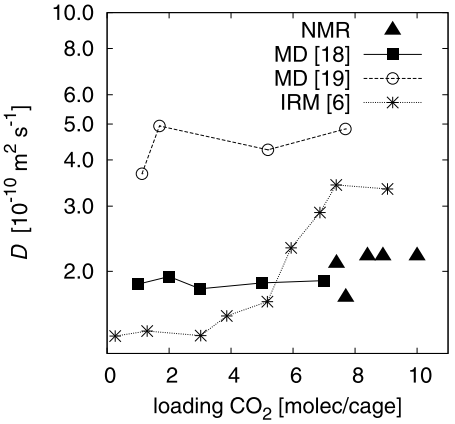


**Fig. 7** Comparison of self-diffusion coefficients of carbon dioxide determined by PFG NMR (▲, this work) with MD simulations (■, Zheng et al. 2012 and ○, Pantatosaki et al. 2012) and IRM data (∗, Bux et al. 2010). The lines serve as guide for the eyes

(Fig. 6) are slightly higher than the previously mentioned MD simulation results and seem to confirm the IRM data at high loadings.

However, the strongly increasing diffusivity for loadings above two methane molecules per cage, which is observed by IRM, is not found in the NMR data. Due to low signal-to-noise ratios, NMR measurements could not be performed in the low loading range, covered by IRM. However, the NMR data exhibit a good signal-to-noise ratio in the high loading range (compare Fig. 4 ) and, therefore, may be considered to be quite accurate in this range. Also, loading dependent MD simulations published for the system methane/ZIF-8 (Pantatosaki et al. 2012; Hertaeg et al. 2011) do not predict strongly increasing self-diffusion coefficients with increasing loading. This is shown in Fig. 6 using our own MD data (more details see Ref. (Pantatosaki et al. 2012)), although these results are about a factor of two faster than the experimental NMR self-diffusion coefficients.

Thus, consolidating the available experimental NMR and IRM data and considering the loading trends predicted by MD simulations, we believe that methane in ZIF-8 exhibits only a slightly increasing self-diffusion coefficient with increasing loading in the range of up to about 4 molecules per cage. Since the IRM diffusivities are actually derived from non-equilibrium measurements and represent Maxwell-Stefan (MS) diffusivities, the larger self-diffusion coefficients at higher loadings point towards possible correlation effects: It might be that a methane molecule is pushed by another molecule through the window of the ZIF-8, while the pushing molecule still remains in the cage where it originated from in the particular diffusion step.

Similar observations as for methane are made for carbon dioxide, if the results of the different methods are compared with each other (see Fig. 7). While the experimental results of IRM and NMR are in the same order of magnitude, they deviate in the loading dependence for loadings above about 5 $CO_2$ molecules per cage. Results of MD simulations agree within the order of magnitude with the experimental results but deviate by a factor of about two from each other. These deviations among the MD simulations are caused by different force fields applied (details see original references (Zheng et al. 2012; Pantatosaki et al. 2012)). However, both MD simulations predict a rather constant self-diffusion coefficient for $CO_2$ in ZIF-8. It should be noted that the MD simulation which is based on an optimized force field obtained via calculation of partial charges of the ZIF-8 framework (Zheng et al. 2012) (denoted by MD (Li et al. 2009) in Fig. 7) shows a very good agreement of the self-diffusion coefficient with the low loading IRM data and the high loading NMR data. Thus, also for carbon dioxide in ZIF-8, we assume that there is rather a constant or only a slightly increasing self-diffusion coefficient with increasing loading in the range to 10 molecules per cage, which correspond to a pressure of about 15 bar in the gas phase.

## 4 Conclusion

In this work, we extended the available experimental data for single component mobilities of adsorbed methane and carbon dioxide in ZIF-8. We reported self-diffusion coefficients of the adsorbed molecules up to loadings of about 4 $CH_4$ molecules and 10 $CO_2$ molecules per cage, respectively, which correspond to pressures in the gas phase of about 15 bar. Additionally, a single measurement for carbon dioxide at 28 bar gas phase pressure (corresponding to about 12 molecules per cage) was performed and found to be in agreement with the loading dependences at the smaller pressures. The measurements, which were carried out by $^1$H

and $^{13}$C PFG NMR, respectively, show that carbon dioxide diffuses slightly faster in ZIF-8 than methane. The ratio between the single component self-diffusion coefficients is $D(CO_2)/D(CH_4) = 1.6 \pm 0.2$ at about 14–15 bar, which means that there is only a slight diffusion separation effect expected. Since in the investigated loading range the single-component self-diffusion coefficients for methane and carbon dioxide obtained by PFG NMR and MD exhibit only a slight loading dependence, we do not expect a significant change of the diffusion separation factor with mixture composition. For example, at an equimolar mixture of a total of 8 molecules per cage, our data yield a ratio of $D(CO_2)/D(CH_4) \approx 1.5$. However this has to be confirmed by binary self-diffusion studies in the future. As recently demonstrated for the MOF CuBTC, such diffusion studies in binary mixtures of $CH_4$ and $CO_2$ can be performed by joint application of $^1$H and $^{13}$C PFG NMR (Schlayer et al. 2012). For the ZIF-8 samples studied here, the corresponding experiments are currently being performed in our laboratory.

At low loadings and pressures, the obtained loading dependences resume the values previously reported by IRM. However, compared to the Maxwell-Stefan diffusivities obtained by IRM, methane and carbon dioxide self-diffusion coefficients in ZIF-8 do not show a significant loading dependence at higher pressures and loadings. This is in good agreement with predictions of MD simulations from different groups. The deviation between the loading dependences observed in the NMR studies under equilibrium conditions and the IRM studies (corrected non-equilibrium data) points towards a correlation effect in the self-diffusion process through the windows of the ZIF-8 framework, in which the molecules e.g. have to push each other when passing through the narrow windows.

**Acknowledgements** The authors would like to thank Friederike Pielenz and the INC Leipzig for the measurement of the high-pressure $CO_2$ adsorption isotherm. We also thank Christian Chmelik for helpful discussions of the loading dependences of the experimental diffusivities.

The research leading to these results has received funding from the European Union Seventh Framework Programme [FP7/2007-2013] under grant agreement no. FP7-NMP-2008-EU-India-233502—AMCOS project. The work was also financially supported by the German Science Foundation through the DFG-SPP 1362 (Porous Metal-Organic Frameworks) and the GK 1056 (Diffusion in Porous Materials).

## References

Aguado, S., Bergeret, G., Titus, M.P., Moizan, V., Nieto-Draghi, C., Bats, N., Farrusseng, D.: New J. Chem. **35**(3), 546 (2011). doi:10.1039/C0NJ00836B

Atci, E., Erucar, I., Keskin, S.: J. Phys. Chem. C **115**(14), 6833 (2011). doi:10.1021/jp200429x

Basu, S., Cano-Odena, A., Vankelecom, I.F.: Sep. Purif. Technol. **81**(1), 31 (2011). doi:10.1016/j.seppur.2011.06.037

Battisti, A., Taioli, S., Garberoglio, G.: Microporous Mesoporous Mater. **143**(1), 46 (2011). doi:10.1016/j.micromeso.2011.01.029

Bux, H., Liang, F., Li, Y., Cravillon, J., Wiebcke, M., Caro, J.: J. Am. Chem. Soc. **131**(44), 16000 (2009). doi:10.1021/ja907359t. PMID: 19842668

Bux, H., Chmelik, C., van Baten, J.M., Krishna, R., Caro, J.: Adv. Mater. **22**(42), 4741 (2010). doi:10.1002/adma.201002066

Bux, H., Chmelik, C., Krishna, R., Caro, J.: J. Membr. Sci. **369**, 284 (2011)

Cotts, R.M., Hoch, M.J.R., Sun, T., Markert, J.T.: J. Mol. Recognit. **83**(2), 252 (1989). doi:10.1016/0022-2364(89)90189-3

Cravillon, J., Schroder, C.A., Bux, H., Rothkirch, A., Caro, J., Wiebcke, M.: CrystEngComm **14**(2), 492 (2012). doi:10.1039/C1CE06002C

Dai, Y., Johnson, J., Karvan, O., Sholl, D.S., Koros, W.: J. Membr. Sci., 76 (2012). doi:10.1016/j.memsci.2012.01.044

Deroche, I., Rives, S., Trung, T., Yang, Q., Ghoufi, A., Ramsahye, N.A., Trens, P., Fajula, F., Devic, T., Serre, C., Ferey, G., Jobic, H., Maurin, G.: J. Phys. Chem. C **115**(28), 13868 (2011). doi:10.1021/jp2039527

Etesse, P., Zega, J.A., Kobayashi, R.: J. Chem. Phys. **97**(3), 2022 (1992). doi:10.1063/1.463139

Fairen-Jimenez, D., Moggach, S.A., Wharmby, M.T., Wright, P.A., Parsons, S., Duìfen, T.: J. Am. Chem. Soc. **133**(23), 8900 (2011). doi:10.1021/ja202154j

Ferey, G., Serre, C., Devic, T., Maurin, G., Jobic, H., Llewellyn, P.L., De Weireld, G., Vimont, A., Daturi, M., Chang, J.S.: Chem. Soc. Rev. **40**(2), 550 (2011)

Ford, D.C., Dubbeldam, D., Snurr, R.Q., Künzel, V., Wehring, M., Stallmach, F., Kärger, J., Müller, U.: J. Phys. Chem. Lett. **3**(7), 930 (2012). doi:10.1021/jz300141n

Hertaeg, L., Bux, H., Caro, J., Chmelik, C., Remsungnen, T., Knauth, M., Fritzsche, S.: J. Membr. Sci. **377**, 36 (2011)

Keskin, S., Liu, J., Johnson, J.K., Sholl, D.S.: Microporous Mesoporous Mater. **125**, 101 (2009)

Li, J.R., Kuppler, R.J., Zhou, H.C.: Chem. Soc. Rev. **38**(5), 1477 (2009)

Liu, D., Zheng, C., Yang, Q., Zhong, C.: J. Phys. Chem. C **113**(12), 5004 (2009). doi:10.1021/jp809373r

Liu, J., Keskin, S., Sholl, D.S., Johnson, J.K.: J. Phys. Chem. C **115**(25), 12560 (2011). doi:10.1021/jp203053h

Pantatosaki, E., Pazzona, F.G., Megariotis, G., Papadopoulos, G.K.: J. Phys. Chem. B **114**(7), 2493 (2010). doi:10.1021/jp911477a. PMID: 20112988

Pantatosaki, E., Megariotis, G., Pusch, A.K., Chmelik, C., Stallmach, F., Papadopoulos, G.K.: J. Phys. Chem. C **116**(1), 201 (2012). doi:10.1021/jp207771s

Park, K.S., Ni, Z., Cote, A.P., Choi, J.Y., Huang, R., Uribe-Romo, F.J., Chae, H.K., O'Keeffe, M., Yaghi, O.M.: Proc. Natl. Acad. Sci. USA **103**(27), 10186 (2006)

Perez-Pellitero, J., Amrouche, H., Siperstein, F., Pirngruber, G., Nieto-Draghi, C., Chaplais, G., Simon-Masseron, A., Bazer-Bachi, D., Peralta, D., Bats, N.: Chem. A Eur. J. **16**(5), 1560 (2010). doi:10.1002/chem.200902144

Rana, M.K., Pazzona, F.G., Suffritti, G.B., Demontis, P., Masia, M.: J. Chem. Theory Comput. **7**(6), 1575 (2011). doi:10.1021/ct100685p

Sant, M., Papadopoulos, G.K., Theodorou, D.N.: J. Chem. Phys. **132**(13), 134108 (2010). doi:10.1063/1.3370344

Schlayer, S., Pusch, A.K., Pielenz, F., Beckert, S., Peksa, M., Horch, C., Moschkowitz, L., Einicke, W.D., Stallmach, F.: Materials **5**(4), 617 (2012). doi:10.3390/ma5040617

Stallmach, F., Galvosas, P.: Annu. Rep. NMR Spectrosc., vol. 61, pp. 51–131. Elsevier, Amsterdam, Boston, Heidelberg (2007)

Stallmach, F., Gröger, S., Künzel, V., Kärger, J., Yaghi, O.M., Hesse, M., Müller, U.: Angew. Chem., Int. Ed. Engl. **45**(13), 2123 (2006). doi:10.1002/anie.200502553

Venna, S.R., Carreon, M.A.: J. Am. Chem. Soc. **132**(1), 76 (2010). doi:10.1021/ja909263x. PMID: 20014839

Wang, B., Cote, A.P., Furukawa, H., O/'Keeffe, M., Yaghi, O.M.: Nature **453**(7192), 207 (2008)

Wehring, M., Gascon, J., Dubbeldam, D., Kapteijn, F., Snurr, R.Q., Stallmach, F.: J. Phys. Chem. C **114**(23), 10527 (2010). doi:10.1021/jp102212w

Yang, Q., Jobic, H., Salles, F., Kolokolova, D., Guillerm, V., Serre, C., Maurin, G.: Chem. A Eur. J. **17**(32), 8882 (2011). doi:10.1002/chem.201003596

Zheng, B., Sant, M., Demontis, P., Suffritti, G.B.: J. Phys. Chem. C **116**(1), 933 (2012). doi:10.1021/jp209463a